ELSEVIER

Biophysical Chemistry 73 (1998) 109–119

Biophysical Chemistry

Time resolved fluorescence properties of phenylalanine in different environments. Comparison with molecular dynamics simulation

J.P. Duneau[a], N. Garnier[a], G. Cremel[b], G. Nullans[b], P. Hubert[b], D. Genest[a], M. Vincent[c], J. Gallay[c], M. Genest[a,*]

[a] *CBM-UPR 4301 du CNRS, affiliated to the University of Orléans, rue Charles Sadron, 45071 Orléans, Cedex 2, France*
[b] *INSERM U.338, 5 rue Blaise Pascal, 67084 Strasbourg, France*
[c] *LURE, Bat 209D, Université Paris-Sud, 91405 Orsay, France*

Received 8 December 1997; received in revised form 26 February 1998; accepted 27 February 1998

Abstract

Time resolved fluorescence of the phenylalanine residue (Phe) alone and included in the transmembrane domain (TMD) sequences of the epidermal growth factor receptor (EGFR) and ErbB-2 was studied using the synchrotron radiation source of light, and compared to molecular dynamics (MD) simulations. The fluorescence intensity decay is strongly sensitive to the environment. A mono-exponential decay was obtained for Phe amino acid alone in two different solvents and for Phe included in EGFR transmembrane sequence, with fluorescence lifetime values varying from 1.7 ns (EGFR) to 7.4 ns (Phe dissolved in water). In ErbB-2 transmembrane sequence three lifetimes were detected. The relative amplitude of the shortest one (0.14 ns) is smaller than 10%, whereas the others (0.6 and 2.2 ns) are almost equally represented. They have been attributed to different rotamers exchanging slowly. This interpretation is supported by MD simulations which evidence transitions in time series of the $\chi 1$ dihedral angle of Phe observed in the case of ErbB-2. The anisotropy decays are similar for both peptides and indicate the presence of a correlation time in the nanosecond range (1–4 ns) and the probable existence of a very fast one (< 0.05 ns). Autocorrelation functions computed from MD simulations corroborate these results.

Keywords: Time resolved fluorescence; Fluorescence of phenylalanine; Molecular dynamics; Transmembrane domains; EGFR; ErbB-2

* Corresponding author.

0301-4622/98/$19.00
PII S0301-4622(98)00142-2

1. Introduction

Helices are widely present in protein structures and are very often viewed as the classical α-helix conformation. However, analysis of helical portions of soluble proteins and a few crystallized membrane proteins reveals structural singularities resulting in distorted rather than straight α-helices [1,2]. Computational studies based on molecular dynamics (MD) simulations confirm the existence of helix deformations [3–5]. In particular, more than sixteen independent runs of 1-ns MD have shown that the transmembrane domain (TMD) of the ErbB-2 oncogenic protein, pertaining to the class I receptor tyrosine kinase (RTK) of the epidermal growth factor receptor (EGFR) family, undergoes conformational transitions between the usual α-helix structure and a conformation bearing π deformations [6–9]. These transitions result in a reorganization of the backbone hydrogen bond (HB) network leading to the disruption of several successive $i \rightarrow i+4$ HB (α-helix) which are replaced by $i \rightarrow i+5$ HB (π-helix). Similar transitions were observed for the wild-type and four different mutated sequences, and the mechanism of transition has been described in detail [8,9]. The resulting structures were found to vary according to the different MD runs, ranging from an almost entire α-helix to an almost entire π-helix. However, the most frequently observed deformations are delimited by specific Gly residues, but this could reflect that 1 ns is an insufficient time scale for completing the transition. Furthermore no correlation was found between the length of the deformation and the nature of the mutation except that replacing the β-branched amino acids by Ala residues inhibits the transition. π structural transitions result in a change in the helix face properties due to π turn-induced rotation about the helix axis. The biological consequences could be of importance in the case of RTK proteins for which receptor dimerization including TMD helix association is necessary for triggering kinase activity [10]. Recent structural studies of ErbB-2 TMD dimer have shown that helices may also undergo π deformation to stabilize helix–helix interactions [7].

Although such unusual portions of π-helices have been experimentally observed in different proteins [1,11], and although it has recently been shown that MD simulation can successfully predict the short time dynamics of oligonucleotides [12] and proteins [13], it is important to get experimental support to confirm the simulation results of the ErbB-2 TMD. The methods of choice for experimental structural studies would be high resolution NMR for the molecule in solution or X-ray crystallography for the molecule in the crystalline phase. Unfortunately, very hydrophobic TMD are often very difficult to crystallize or to dissolve at concentrations necessary for NMR studies. Other biophysical techniques are also able to give structural or dynamical information about proteins, but with a much lower resolution. Among them, many transient fluorescence spectroscopy studies of the fluorescent amino acid tryptophan have been reported, including the determination of rotational correlation times by using linearly polarized light, which allows to explore the internal dynamics of macromolecules [14,15].

To a lesser extent, the tyrosine amino acid has also been used for small protein dynamics estimation, and it has particularly been shown that the different fluorescence lifetimes of this residue are related to the three rotamers characterized by different values of the $\chi 1$ angle of its side chain [16–18].

The molecules we are interested in do not bear any Trp or Tyr residues but one Phe residue is present. This residue is another fluorescent amino acid naturally present in proteins, but its fluorescence has almost never been used because it is very weak and screened by that of Trp or Tyr residues. Furthermore the number of Phe residues is generally important in proteins so that individual Phe cannot be identified. Statistically, one or two Phe residues are found in the TMD of class I membrane proteins [19]. One can wonder whether the weak fluorescence of this amino acid can be used to monitor the structural behavior of such peptide sequences when no Tyr or Trp are present. Unfortunately, very few data are available in the literature [20–22] and before expecting to get

structural or dynamical information, the fluorescence of Phe must be investigated more deeply.

The first goal of the present prospective study is to explore whether the synchrotron radiation source of light can be used to measure fluorescence lifetimes and anisotropy decay parameters of Phe under different conditions of solvent for this chromophore alone or included in peptide sequences. The results obtained from this time resolved fluorescence study are reported, either for the free amino acid dissolved in water or in a 2:1 mixture of chloroform/methanol ($CHCl_3$/MeOH), or embedded in two peptide sequences corresponding to the wild EGFR TMD and to the Glu659 mutant of ErbB-2 TMD dissolved in $CHCl_3$/MeOH. These two peptides used in fluorescence experiments are named EGFRtm and ErbB-2*tm, respectively.

The second goal was to calculate from the available MD trajectories [8] relevant quantities that could be related to the fluorescence experiments in order to check if the comparison between both techniques can be considered. Such a comparison has already been done for Trp in proteins [23]. The quantities examined here are the $\chi 1$ dihedral angle fluctuations of Phe in the Glu^{659} mutant of ErbB-2 TMD, and the second Legendre polynomials of the Cγ-Cζ vector autocorrelation function of the phenyl ring. For the first case three independent MD runs leading to a total of 2.5 ns were used, and for the second case sixteen 1-ns MD runs corresponding to different mutants of ErbB-2 TMD were analyzed. The first quantity is related to the fluorescence intensity decay and the second one to the fluorescence anisotropy decay.

2. Materials and methods

2.1. Molecular dynamics simulations

The present study uses the trajectories of 16 independent 1-ns simulations of 29-residue peptides having the wild sequence of ErbB-2 TMD or different mutated sequences. MD simulations were performed *in vacuo* using the GROMOS [24] or XPLOR [25] packages. The detailed MD protocol was described by Duneau et al. [9]. The overall motion of the molecules was removed by fitting each instantaneous conformation to the initial one. The wild-type sequence is LTSII-SAVV^{659} GILLVVVLGVVFGILIKRRQ and it has been simulated two times. This concerns the sequence 651–679 of the whole protein. Four mutants correspond to the mutations of Val^{659} by Gly^{659} (five simulations), Glu^{659} (three simulations), Gln^{659} (two simulations) and Asp^{659} (two simulations). Two simulations were also carried out on an additional sequence in which all Val residues of the Gly^{659} mutant have been replaced by Ala residues. From all trajectories, the time series of the Phe $\chi 1$ dihedral angles were calculated.

The normalized autocorrelation function describing the reorientation of the Phe residue within the peptide was numerically calculated for each simulation as:

$$C(k\cdot\Delta t) = \{3\langle\cos^2\phi(k\cdot\Delta t)\rangle - 1\}/2$$

In this expression Δt is the time interval between successive configurations (0.4 ps), and $\phi(k\cdot\Delta t)$ is the angle between the directions of the $C\gamma$-$C\zeta$ vector of Phe ring at times 0 and $k\cdot\Delta t$, respectively. The angle brackets represent the average over all the possible orientations at time 0 and $k\cdot\Delta t$ was allowed to vary from 0–0.1 ns. In order to improve the statistical accuracy, an additional averaging of the $C(k\cdot\Delta t)$ functions was performed over simulations giving the same mean structure (this will be explained in the result section). The choice of the $C\gamma$-$C\zeta$ vector for describing the reorientation of the phenyl ring was guided by reasons of symmetry but this vector does not necessarily match the direction of the emission dipolar moment.

2.2. Sample preparations

The EGFRtm peptide was furnished by Neosystem (Strasbourg, France). The ErbB-2*tm was obtained by a solid phase peptide synthesis using the Fmoc strategy with a SYNERGY synthetiser (Applied Biosystem 432A). Both peptides were purified by reverse phase HPLC using a C4, nucleosyl 300-7, Machery–Nagel column (Dueren,

Germany). All the buffers used contained 1% of trifluoroacetate. The peptides were dissolved in solution A (Isopropanol:Acetonitrile 1:2). After washing with a buffer containing 95% water and 4% solution A, the peptides were eluted using a linear gradient of solution A from 4% to 70%. Peaks were analyzed by mass spectroscopy. The sequences of the purified peptides were determined using an Applied Biosystem 473A microsequencer.

The sequences of both peptides are:

EGFRtm

SIATGMVGALLLLLVVALGIGLFMR,

ErbB-2*tm

DSMLTSIISAVEGILLVVVLGVVFLILIKRR.

EGFRtm and ErbB-2*tm were dissolved in a $CHCl_3$/MeOH mixture (2:1 ratio vol. to vol.) at an initial concentration of 4×10^{-4} M and 3×10^{-4} M, respectively. After sonication, the major part of the peptides was solubilized. However, after a short time, aggregates are observed leading to a sedimentation process. The solutions were centrifuged (20 min at 10 000 rpm) and the supernatents were used for experiments. Nevertheless, aggregated forms reappeared with time giving rise to solutions with some turbidity but with no additional sedimentation. Under these conditions, the final concentrations are low and only poorly defined.

For EGFRtm, fluorescence experiments were performed with the mother solution and with a five times dilution. For ErbB-2*tm, experiments have been done with two samples corresponding to two times and four times dilution of the mother solution.

2.3. Fluorescence spectroscopy

Emission spectra, excitation spectra and steady state anisotropy were measured with a SLM 8000 spectrofluorometer. For the excitation anisotropy spectrum the emission wavelength was 290 nm.

Fluorescence intensity and anisotropy decay data were obtained on the time-resolved spectrofluorometer installed on the SB1 line of the storage ring Super-ACO (Anneau de Collision d'Orsay) which provides an ~ 0.5-ns light pulse at a frequency of 8.33 MHz for the two-bunch mode. The instrument uses the time-correlated single-photon counting method. It is fully automatic (motorized excitation and emission monochromators, emission polarizer and four-position temperature-controlled sample turret) driven by a PC microcomputer. The instrument response function $E_\lambda(t)$ was monitored at the emission wavelength using a scattering glycogen solution, alternatively with the polarized fluorescence decays and the corresponding blanks when needed. The data was stored in a MCA 2K memories (Canberra France) and processed on a Vax station 4000/90. The time resolution was ~ 17 ps per channel and the acquisitions were stopped when approx. 20 000 counts were stored at the top of the vertical component. The excitation and emission wavelengths were 254 nm and 290 nm, respectively, and all the experiments were performed at 20°C.

Fluorescence intensity decay data analysis was performed by the Maximum Entropy Method (MEM) [26,27] using the commercially available library of subroutines MEMSYS 5 (MEDC Ltd., UK). This analysis does not assume either the number of components, or the width of each lifetime distribution. Both are the result of the analysis, which essentially depends on the signal-to-noise ratio. It is worth emphasizing that all the analyses started from the first channel for which the fluorescence signal was above the noise level. Lifetime components as short as ~ 20 ps can be recovered with this instrument.

For the determination of the total intensity decay parameters, the vertical and twice the corrected horizontal components of the polarized light were summed:

$$T(t) = I_{VV}(t) + 2\epsilon_{\text{corr}} I_{VH}(t)$$
$$= E_\lambda(t) * \int_0^\infty \alpha(\tau)\exp(-t/\tau)d\tau \quad (1)$$

where ϵ_{corr} is a correction factor for the differential transmission by the emission monochromator of the two polarized light components [28]. $\alpha(\tau)$ is the lifetime distribution.

The center τ_j of a single class j of lifetimes

over the $\alpha(\tau_j)$ distribution is defined as:

$$\tau_j = \frac{\sum_i \alpha(\tau_i)\tau_i}{\sum_i \alpha(\tau_i)} \quad (2)$$

the summation being performed on the significant values of the $\alpha(\tau_i)$ for the j class. α_j is the normalized contribution of the lifetime class j.

Polarized fluorescence emission decays were analyzed by MEM assuming that all the excited state populations display the same rotational properties. Then, the polarized components were written as:

$$I_{VV}(t) = \tfrac{1}{3}E_\lambda(t) * \int_0^\infty \alpha(\tau)\mathrm{e}^{-t/\tau}d\tau \times \left[1 + 2\int_0^\infty \beta(\theta)\mathrm{e}^{-t/\theta}\mathrm{d}\theta\right] \quad (3)$$

and

$$I_{VH}(t) = \tfrac{1}{3}E_\lambda(t) * \int_0^\infty \alpha(\tau)\mathrm{e}^{-t/\tau}\mathrm{d}\tau \times \left[1 - \int_0^\infty \beta(\theta)\mathrm{e}^{-t/\theta}\mathrm{d}\theta\right] \quad (4)$$

with

$$r_0 = \int_0^\infty \beta(\theta)\mathrm{d}\theta \quad (5)$$

where θ is the rotational correlation time with distribution $\beta(\theta)$, r_0 is the fluorescence anisotropy at time 0 and the other symbols have the same significance as in Eq. (1). The $\alpha(\tau)$ profile is given from a first analysis of $T(t)$ by MEM and is held constant in a subsequent and concomitant analysis of $I_{VV}(t)$ and $I_{VH}(t)$ which provides the distribution $\beta(\theta)$ of correlation times. One hundred rotational correlation time values, equally spaced in logarithmic scale and ranging from 0.01 to 10 ns were used for the analysis of $\beta(\theta)$.

The barycenters of the correlation time distribution were calculated as:

$$\theta_j = \frac{\sum_i \beta_i(\theta_i)\theta_i}{\sum_i \beta_i(\theta_i)} \quad (6)$$

β_i being the contribution of the rotational correlation time i to the class j.

According to [23] the fluorescence anisotropy decay $r(t)$ of a fast rotational motion with limited amplitude and characterized by a single correlation time θ tends to a plateau value r_∞ at long times and can be written as:

$$r(t) = (r_0 - r_\infty)e^{-t/\theta} + r_\infty \quad (7)$$

3. Results

3.1. Fluorescence lifetimes

Table 1 summarizes all the results of the fluorescence decay of the Phe residue in different conditions.

3.1.1. Free amino acid

We found a single exponential decay for the free amino acid. However, the lifetime is strongly dependent on the solvent since in $CHCl_3$/MeOH ($\tau = 3.55$ ns) the fluorescence is quenched by a factor of 2 relatively to Phe dissolved in water

Table 1
Fluorescence decay parameters at T = 20°C of the free Phe amino acid, EGFRtm and ErbB-2*tm dissolved in water (a) and in 2:1 $CHCl_3$/MeOH mixture (b-f) at different dilutions: (c), (e); higher concentration; (d), (f) lower concentration (see text).

Experiment	$\alpha 1$	$\tau 1$	$\alpha 2$	$\tau 2$	$\alpha 3$	$\tau 3$	$\langle\tau\rangle$
(a) Phe	1.0	7.40	—	—	—	—	7.40
(b) Phe	1.0	3.55	—	—	—	—	3.55
(c) EGFRtm	1.0	1.74	—	—	—	—	1.74
(d) EGFRtm	1.0	1.69	—	—	—	—	1.69
(e) ErbB-2*tm	0.10	0.16	0.45	0.63	0.45	2.20	1.31
	0.009	0.15	0.46	0.65	0.45	2.27	1.33
(f) ErbB-2*tm	0.008	0.12	0.38	0.55	0.54	2.16	1.40

Notes: Two experiments were performed for (e). Times are given in ns.

($\tau = 7.4$ ns). This last value is close to the value of 6.8 ns determined by Leroy et al. [20].

3.1.2. EGFRtm

The fluorescence of Phe in EGFRtm dissolved in $CHCl_3$/MeOH is also characterized by a single exponential decay (Fig. 1a) with a fluorescence lifetime in the order of 1.7 ns. Therefore the fluorescence is also quenched by a factor of 2 relative to the free amino acid Phe in the same solvent. Identical results were obtained for two different concentrations of the peptide.

3.1.3. ErbB-2 * tm

On the contrary, the fluorescence decay of ErbB-2*tm is a sum of three exponential terms (Fig. 1b). For the three experiments that were performed, the mean lifetime has approximately the same value (~ 1.34 ns), which is significantly smaller than the single lifetime found in the case of EGFRtm. Within the experimental accuracy, the three experiments exhibit essentially identical decays which do not depend on the concentration. A small proportion ($< 10\%$) of a short lifetime of 0.14 ns is found. The longest lifetime obtained for the peptide at both concentrations is 2.2 ns. The different experiments give a proportion of approx. 0.48 for this long time component. Finally an intermediate lifetime of 0.60 ± 0.05 ns was detected with a proportion of 0.43. None of the lifetime values found in ErbB-2*tm was observed in EGFRtm.

3.2. Fluorescence anisotropy

3.2.1. Steady state anisotropy

Fig. 2 shows the steady state anisotropy of the free amino acid Phe dissolved in the mixture glycerol-H_2O (90/10 w/w) at -55°C as a function of the excitation wavelength. Between 250 nm and 265 nm a plateau is observed. It can be seen that the anisotropy is very weak in the order of 0.065. Under our experimental conditions all molecular motions are expected to be suppressed, so that the measured anisotropy corresponds to the fundamental anisotropy r_0. Assuming that such a small value is caused by the non-colinearity between the excitation and emission transition dipoles, the angle between both these vectors is approx. 50°.

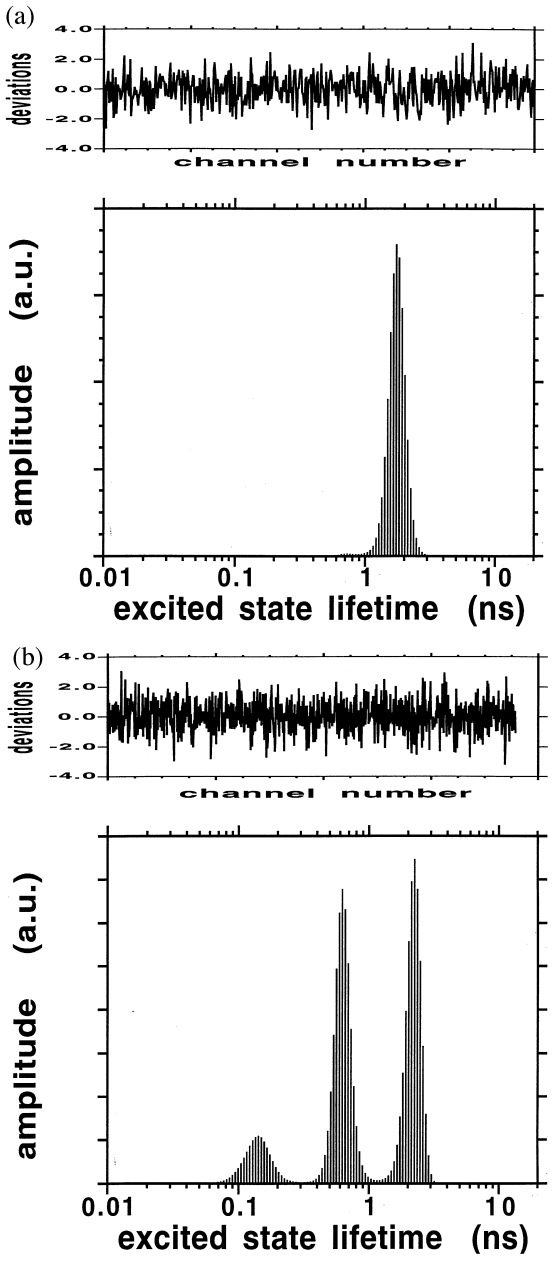

Fig. 1. Distribution of fluorescence lifetimes for the higher concentration of EGFRtm (a) and ErbB-2*tm (b). Upper parts: RMS deviation between experimental and recalculated decay.

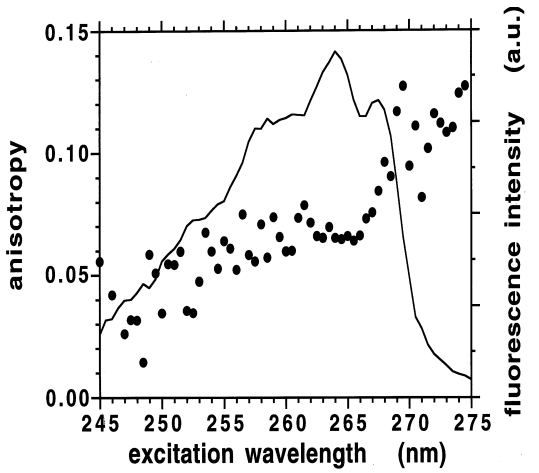

Fig. 2. Exitation (continuous line) and steady state fluorescence anisotropy (filled circles) spectra of Phe in 90/10 w/w glycerol/H_2O at -55°C. Emission wavelength was 290 nm.

3.2.2. Anisotropy decay

The fluorescence anisotropy decays of ErbB-2*tm and EGFRtm were only poorly resolved, due to the low signal/noise ratio of the experimental curves and to the low value of r_0. Thus an accurate analysis cannot be presented. In these conditions it is impossible to evidence a difference between the anisotropy decays of both peptides, but this does not mean that no difference exists. However, common features are observed for all the experiments: (1) all the decays are reasonably correctly fitted by the sum of a single exponential term and of a constant term r_∞ ; (2) the anisotropy at time 0 ($r_{t=0}$) is smaller than the fundamental anisotropy r_0. The plateau value r_∞ is 0.02 ± 0.01 and the value of $r_{t=0}$ is 0.035 ± 0.010. The single rotational correlation time was found to vary between 1 and 4 ns. The r_∞ value indicates a strongly restrained motion in the nanosecond range compatible with oligomerization, and the low $r_{t=0}$ value seems to indicate the existence of very fast motions (faster than ~ 50 ps with the time resolution of our apparatus).

3.3. MD simulations of different mutants of ErbB-2 TMD

3.3.1. Phe rotamers in the Glu^{659} mutant of ErbB-2 TMD

Fig. 3 gives an example of the time series of the

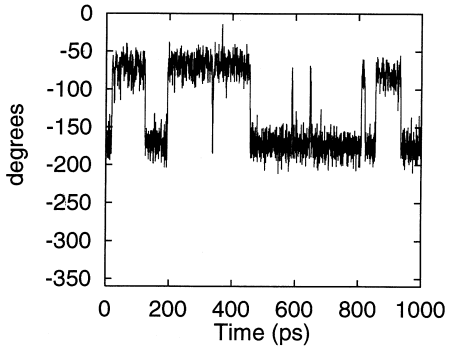

Fig. 3. Example of time series of $\chi 1$ dihedral angle of Phe in the Glu659 mutant of ErbB-2 TMD obtained from MD simulation.

$\chi 1$ dihedral angle of the Phe residue in the Glu^{659} mutant of ErbB-2 TMD, as obtained from one of the MD simulation performed in absence of solvent. The same behavior is observed for the two other independent simulations. Transitions between two rotamers are observed corresponding to $\chi 1 = -60°$ and $-180°$, respectively. The third possible rotamer $\chi 1 = +60°$ is not observed. On the average a transition occurs every 0.1 ns and both rotamers are almost equally populated with 58% for $\chi 1 = -60°$ and 42% for $\chi 1 = -180°$. Similar results are obtained for the other mutants (not shown).

3.3.2. Computed internal anisotropy decay

The normalized rotational autocorrelation functions related to the internal component of the fluorescence anisotropy were calculated for each of the 16 simulations (see materials and methods). Owing to the limited number of $\chi 1$ transitions occurring in 1 ns (see Fig. 3), no statistical accuracy can be reached for any of the calculated curves. However, one observes a tendency for the autocorrelation functions to depend on the helix structure and not on the nature of the mutants. In particular the participation or not of the Phe residue to a π deformation seems to be important. The whole set of trajectories can be classified according to the resulting helical structures. Four classes are defined as follows: (1) the structure is a canonical α-helix; (2) a short π bulge (< 5 $i \rightarrow i + 5$ HB) is present in the α-helix

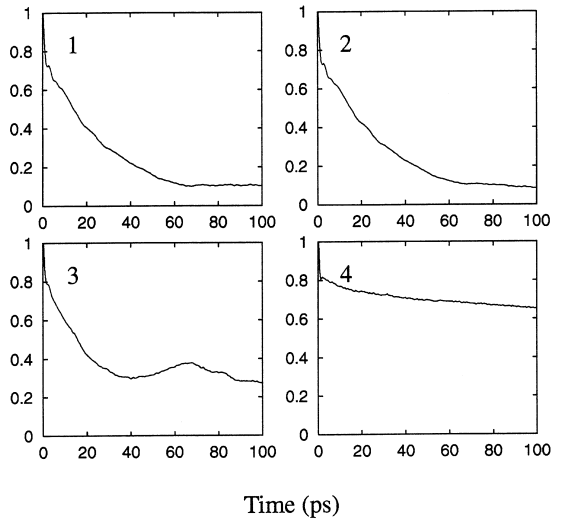

Fig. 4. Normalized autocorrelation functions of the Cγ-Cζ vector of Phe calculated from 16 independent 1-ns MD simulations in different ErbB-2 TMD sequences (wild and mutated). The labels of the four curves correspond to the different classes of conformations defined in the text.

and Phe is not embedded in the π bulge; (3) the helix exhibits a longer π deformation (6–15 $i \rightarrow i + 5$ HB) in which Phe participates to the π HB pattern only by its NH group; and (4) the structure is almost a full π-helix in which Phe is fully involved. For each trajectory of a class, the autocorrelation functions have been calculated over 100 ps and subsequently averaged. The four resulting curves are displayed in Fig. 4. A common feature is a very fast initial decay in less than 1 ps from 1 to approx. 0.75 ± 0.05. This reflects a very fast libration of the phenyl ring with an amplitude of approx. 24°. This motion corresponds to $\chi 1$ dihedral angle fluctuations about its mean value for each of the rotamers. Then a slower decay is observed. Anisotropies from classes 1 and 2 reach a plateau value at 0.1 after 50 ps. For the middle-size π deformation (class 3) a plateau at 0.3 is reached after approx. 30 ps. The autocorrelation functions of the full π-helix decreases much more slowly, and even after a time delay of 100 ps a plateau is not reached and a value as high as 0.65 is found.

4. Discussion

4.1. Simulation

MD simulations of the wild ErbB-2 TMD and of its few mutants reveal that Phe is labile. First an exchange between two $\chi 1$ rotamers is observed during the time course of the simulation. Then the Cγ-Cζ vector autocorrelation function decays in a two-step process primarily from 1 to approx. 0.75 in < 1 ps then from 0.75 to a value between 0.1 and 0.65 during the following 100 ps, depending upon the conformation of the peptide. It is found that the fast initial decay is caused by the fluctuations of $\chi 1$ about the equilibrium position for each of both rotamers. The slower decay of the autocorrelation functions is less obvious to interpret owing to its dependance upon the $\chi 1$ transitions but also upon the deformations of the rest of the molecule. Nevertheless this MD study shows that the Phe ring in a π-helix is much more rigid than in the α-helix.

4.2. Fluorescence

The fluorescence intensity decay of Phe is strongly dependent upon the environment. A single lifetime is found for the free amino acid in water and in $CHCl_3$/MeOH or for the amino acid located near the C-terminus of EGFRtm, but is different in the three cases. In water the fluorescence is twice higher than in $CHCl_3$/MeOH and four times greater than in EGFRtm. On the contrary, two main components with approximately equal population are present in the fluorescence decay of ErbB-2$*$tm and a third one is also observed but with a very low proportion ($< 10\%$). It is obvious that some aggregates were present in the samples but they do not seem to introduce artefacts in the decay analysis, a good reproducibility of the experiments being obtained at the two different concentrations. None of the lifetimes found in ErbB-2$*$tm is similar to that of the free chromophore or of Phe in EGFRtm. The fluorescence properties of Phe in ErbB-2$*$tm can be compared to those of the Tyr or O-methyl-Tyr residues determined in different peptides for which three fluorescence lifetimes are also

observed [16–18]. In the case of Tyr each lifetime has been attributed to each of the three $\chi 1$ rotamers. If the exchange rate between the rotamers is slower than the lifetime of the excited state, the three fluorescence lifetimes are present in the decay. The same assumption can be made for Phe in ErbB-2*tm, and the three lifetimes observed mean that transitions between different rotamers occur with a slow exchange rate compared to the lifetime of the excited state (>10 ns).

It is found that the most quenched rotamer is poorly populated so that its contribution to the total fluorescence intensity is smaller than 2%. Slow exchange rate between rotamers suggests hindered rotational motions of the Phe side chain which could result from intramolecular or intermolecular interactions. It has not been possible to discriminate between both possibilities because the range of concentrations which can be used is too small owing to difficulties of solubilization and to the weak fluorescence of Phe. The assumption of a relationship between lifetimes and rotamers is supported by MD simulations which evidence transitions between rotamers both in the monomeric or dimeric (not shown) forms of this peptide. In the simulations performed in vacuo during 2.5 ns, only the two rotamers $\chi 1 = -60°$ and $\chi 1 = -180°$ are observed. The same observation holds for all the mutants which were simulated. This suggests that the rotamer $\chi 1 = +60°$ is not found neither in the α-helix, nor in the π-helix. This finding is consistent with the fact that the fluorescence decay exhibits mainly two lifetimes (more than 90% of the whole decay) in approximately equal proportions. The fact that the rate exchange is fast in the simulation (~ 0.1 ns) is partly due to the absence of explicit solvent molecules, and damping effects are expected to occur in a real experiment.

The fluorescence emission of Phe in EGFRtm is characterized by a single exponential decay. If the above hypothesis which attributes the lifetimes to different rotamers is correct, then either the rotamers exchange rapidly in this peptide or only one rotamer is present. Both these possible causes express two opposed behavior since the first one characterizes a great freedom of rotation whereas the second one characterizes hindered motions. Examination of the sequences of both peptides is in favour of the first hypothesis. Indeed Phe is near the C-terminal extremity of EGFRtm so that it is expected to be more flexible than in ErbB-2*tm where it is located in the core of the sequence. However, the fluorescence lifetime in EGFRtm is two times smaller than for the free amino acid in the same solvent, indicating that in this peptide, Phe is not fully accessible to the solvent.

The fluorescence anisotropy decays were difficult to measure, arising: (1) from the existence of aggregates in the samples; (2) from the very low fundamental anisotropy r_0 giving rise only to a small variation range of the decay for determining correlation times; and (3) from the very weak recorded signal.

The observation of a value of 0.02 for the long time anisotropy r_∞ is possible only if both the overall motion of the molecule and the internal deformations are limited in space, but their relative contribution cannot be established. The most simple interpretation is that during the time a chromophore remains in the excited state (no more than 10 ns), the whole molecule does not move significantly, so that the experimental decay is due only to limited internal motions of the Phe residue. Limited overall motion could be, at least partially, a consequence of aggregation. The interpretation of the limited internal deformation is more ambiguous and at least two different hypotheses can be invoked: (1) independently of the peptide conformation, the motions are hindered by intermolecular contacts within aggregates; or (2) the individual molecules adopt a conformation with slow internal dynamics. For example, MD simulations have shown that the presence of π-helix portions slows down the decay of the reorientational correlation function of the Phe side chain. These two possibilities do not preclude each other. Although an accurate analysis of the anisotropy experiments is not available, data are qualitatively in good agreement with simulation results. Both techniques show the existence of a very fast motion in less than a few picoseconds

which is attributed to the fast $\chi 1$ fluctuations of each rotamer, followed by a much slower motion characterized by a correlation time in the order of tens of picoseconds for in vacuo simulation and in the order of a few ns for fluorescence experiments. This slower decay is related to the different internal motions of the peptides, and particularly to the transitions between the two rotamers of the Phe residue. No more precise information about the relationship between the rotamers and the anisotropy decay can be given.

Very few studies have been devoted to the fluorescence of Phe in peptides or proteins. Sudhakar et al. [22] have reported fluorescence lifetimes of Phe residues in cod fish parvalbumin type II in aqueous solvent, a protein which contains no Trp and no Tyr, but 10 Phe. Two lifetimes were found but their relative populations could not be determined. One of them was surprisingly long (53 ns) in the native protein but decreases to 17 ns after denaturation, which is about twice the value of the free residue dissolved in water. These results are very different from those presented in this work since we do not observe such long fluorescence lifetimes.

5. Conclusion

The present study shows that the synchrotron radiation source of light allows us to detect and analyze the transient fluorescence of Phe in peptides. We have shown that the fluorescence lifetimes are strongly dependent on the environment. In particular the expression of the intensity decay can bring information on the internal dynamics of the peptides. This allows comparisons between different sequences or different states of a same peptide. In spite of the low fundamental anisotropy of Phe and of the presence of aggregates of the transmembrane peptides studied in this work, it has been possible to extract qualitative information from the fluorescence anisotropy decay.

The comparison between these experiments and MD simulations was undertaken for the Glu659 mutant of the ErbB-2 TMD and a qualitatively good agreement was obtained in the interpretation of the intensity fluorescence decay. We believe that quantitative agreements will be obtained in the future by including explicitly the solvent in the simulations as it is now possible with the development of computers. On the contrary, the comparison between the results of MD simulations and of anisotropy decay is more difficult, because the experimental data are not sufficiently accurate and can be interpreted in different ways. However, even in this case both techniques give consistent data.

Finally the simulation gives an interesting insight into the role of ErbB-2 TMD conformation on its internal dynamics. It is shown that π deformations rigidify strongly the molecule, at least at the level of the Phe residue. In order to verify experimentally this prediction without ambiguity, better conditions of peptide solubilization have to be found. Such prospection is in progress in our laboratory.

Acknowledgements

This work was supported by a grant from the French 'Association de la Recherche contre le cancer (ARC)'.

References

[1] K.R. Rajashankar, S. Ramakumar, Protein Sci. 5 (1996) 932–946.
[2] D.J. Barlow, J.M. Thornton, J. Mol. Biol. 201 (1988) 601–619.
[3] D. van der Spoel, B.L. de Groot, S. Hayward, H.J.C. Berendsen, H.J. Vogel, Protein Sci. 5 (1996) 2044–2053.
[4] L.K. Iyer, S. Vishveshwara, Biopolymers 38 (1996) 401–421.
[5] I.D. Kerr, H.S. Son, R. Sankararamakrishnan, M.S. Sansom, Biopolymers 39 (1996) 503–515.
[6] N. Garnier, D. Genest, E. Hebert, M. Genest, J. Biomol. Struct. Dyn 11 (1994) 983–1002.
[7] N. Garnier, D. Genest, J.P. Duneau, M. Genest, Biopolymers 42 (1997) 157–168.
[8] J.P. Duneau, N. Garnier, M. Genest, J. Biomol. Struct. Dyn. 15 (1997) (in press).
[9] J.P. Duneau, D. Genest, M. Genest, J. Biomol. Struct. Dyn. 13 (1996) 753–769.
[10] C.H. Heldin, Cell 80 (1995) 213–223.
[11] B.J. Gaffney, Annu. Rev. Biophys. Biomol. Struct. 25 (1996) 431–459.
[12] F. Gaudin, D. Genest, G. Lancelot, Eur. Biophys. J. 26 (1997) 239–245.
[13] M. Philippopoulos, A.M. Mandel, A.G. Palmer III, C. Lim, Proteins 28 (1997) 481–493.

[14] O.P. Kuipers, M. Vincent, J.C. Brochon, H.M. Verheij, G.H. De Haas, J. Gallay, Biochemistry 30 (1991) 8771–8785.
[15] N. Rouvière, M. Vincent, T. Craescu, J. Gallay, Biochemistry 36 (1997) 7339–7352.
[16] W.R. Laws, A.J.B. Ross, H.R. Wyssbrod, J.M. Beechem, L. Brandt, J.C. Sutherland, Biochemistry 25 (1986) 599–607.
[17] A.J.B. Ross, W.R. Laws, A. Buku, J.C. Sutherland, H.R. Wyssbrod, Biochemistry 25 (1986) 607–612.
[18] I. Harnois, D. Genest, J.C. Brochon, M. Ptak, Biopolymers 27 (1988) 1403–1413.
[19] C. Landolt-Marticorena, K.A. Williams, C.M. Deber, R.A. Reithmeier, J. Mol. Biol. 229 (1993) 602–608.
[20] E. Leroy, H. Lami, G. Laustriat, Photochem. Photobiol. 14 (1971) 411–421.
[21] E.A. Permyakov, E.A. Burstein, Biophys. Chem. 19 (1984) 265–271.
[22] K. Sudhakar, W.W. Wright, S.A. Williams, C.M. Phillips, J.M. Vanderkooi, J. Fluorescence 3 (1993) 57–64.
[23] T. Ichiye, M. Karplus, Biochemistry 22 (1983) 2884–2893.
[24] W.F. van Gunsteren, H.J.C. Berendsen, GROMOS 87 package; BIOMOS Biomolecular Software, University of Groningen, 1986.
[25] A.T. Brunger, *X-PLORManual*", Yale University, 1992.
[26] A.K. Livesey, J.C. Brochon, Biophys. J. 52 (1987) 693–706.
[27] J.C. Brochon, Methods Enzymol. 240 (1994) 311–362.
[28] P. Wahl, Biophys. Chem. 10 (1979) 91–104.